

X-ray analysis of the device structures of III-V compound semiconductors

Mai Zhen-hong, Cui Shu-fan, and He Chu-guang

Institute of Physics, Academia Sinica, P.O. Box 603, Beijing 100080, People's Republic of China

(Received 1 August 1989; revised manuscript received 20 November 1989)

A computer program for the simulation of the x-ray double crystal rocking curves of arbitrary epitaxial structures was established based on x-ray dynamical diffraction theory. Uniformly single-layer, waveguide structures and laser structures as well as superlattices were examined experimentally and theoretically. The theoretical results are in excellent agreement with the experimental ones. For the laser double heterostructures (ABA), the uniformities of the active layer B can be obtained from the variation of the fine structures of the diffraction peaks of A layers. In the studies of quantum-well structures we concluded that there exists incoherent growth in the interface of the specimen where 50% of the epitaxial layers are relaxed. These results are significant for improving quality and growth condition of device structures of III-V compound semiconductor materials.

I. INTRODUCTION

The structural parameters of epitaxial materials can be measured by means of a variety of methods, such as x-ray double crystal diffraction, Raman spectroscopy, and electron diffraction, etc. Among them the x-ray double crystal diffraction, which is considered a highly accurate and nondestructive testing method, has become an ordinary and effective tool.

The physical information given by double crystal diffraction is included in the rocking curves. Except in a few cases, for example, for a very thin or simple epitaxial layer, kinematical theory cannot generally give proper results. As the layer structures become complicated, the separation of diffraction peaks does not correspond to the differences of lattice constants. The diffraction profile can be influenced by all the structural parameters, so that the kinematical analysis often leads to incorrect results. A semikinematical approximation was first introduced by Petrashen^{1,2} and somewhat later it was employed to study the strain profile induced by the distribution of the impurities and defects in single crystals of silicon.^{3,4} Tapfer and Ploog used it to simulate the rocking curves of epitaxial-layer structures.⁵ The semikinematical diffraction theory can provide more accurate results than kinematical theory but gives rise to considerable errors for systems with large lattice mismatch.

The simulation based upon the dynamical theory was also developed from the studies of strain profile induced by ion-implantation and boron diffusion.⁶⁻⁸ Recently, a lot of theoretical and experimental studies were performed in the background of the rapid development of optic and electric devices with epitaxial materials,⁹⁻¹¹ indicating that the dynamical simulation is a very effective method for studying the structures of epitaxial layers.

In the present paper based on x-ray dynamical theory the reflection coefficients of epitaxial structures were derived. Some device structures of III-V compound semi-

conducting materials were investigated with computer simulation.

II. THE REFLECTION COEFFICIENTS FOR ARBITRARY EPITAXIAL STRUCTURES

Defining the complex reflecting coefficient

$$Q = \left[\frac{|\gamma_h|}{\gamma_0} \right]^{1/2} \frac{D_h}{D_0}, \quad (1)$$

we can obtain the following equation⁹ deduced from Taupin's expressions:¹²

$$Q_{k+1} = \frac{Q_k S + i(E + BQ_k)\tan(DSt_k)}{S - i(B + AQ_k)\tan(DSt_k)}, \quad (2)$$

where

$$\begin{aligned} D &= \frac{\pi}{\lambda} \left[\frac{|\gamma_h|}{\gamma_0} \right]^{1/2}, \\ A &= C \frac{\chi_h}{|\gamma_h|}, \\ B &= \frac{1}{2} \left[\frac{\gamma_0}{|\gamma_h|} \right]^{1/2} \left[\frac{\chi_0}{\gamma_0} + \frac{\chi_0}{|\gamma_h|} - \frac{\alpha_h}{|\gamma_h|} \right], \\ E &= C \frac{\chi_h}{|\gamma_h|}, \end{aligned} \quad (3)$$

$$\alpha_h = -2(\theta - \theta_B)\sin 2\theta_B,$$

$$S = \left[B^2 - EA \right]^{1/2},$$

$$t_k = Z_{k+1} - Z_k.$$

For infinitely thick crystals one can obtain

$$Q = - \frac{B + S \operatorname{sgn}(\operatorname{Im}S)}{A}. \quad (4)$$

Equation (2) represents the successive relationship of two contiguous layers. Therefore starting from the interface between the substrate and the epitaxial layers utilizing Eq. (2) we can yield the reflecting coefficient at the surface of specimens whose complex square will be the reflectivity. The substrate can be treated as an infinitely thick crystal, thereby the reflecting coefficient at the interface can be deduced from Eq. (4). The convolutions of reflectivities between the first and the second crystal are needed in order to make comparison with experiments.

In the above derivations no assumption has been made concerning the structures along the Z direction (the surface normal) in the epitaxial layers so that Eq. (2) is applicable to arbitrary epitaxial structures provided that all the parameters needed in Eq. (2) such as χ , θ_B , γ_0 , γ_h and α_h , etc. are defined as a function of the ordinate Z.

III. THE X-RAY ANALYSIS OF THE DEVICE STRUCTURES OF III-V COMPOUND SEMICONDUCTORS

To confirm the universality of the theoretical results above, rocking curves of several device structures were investigated and compared with the experimental ones. In this section, a (001) GaAs slice was used as the first crystal and 004 reflection was accepted in all of the x-ray double crystal diffraction experiments, except where otherwise stated.

A. Uniform single layer

The simplest epitaxial structure is the so-called uniform single layer, for example, single heterostructure of $Ga_{1-x}Al_xAs$ on GaAs or $In_xGa_{1-x}As$ on InP. The rocking curves in connection with uniformly single heterostructures are relatively simple; they include two peaks, one the reflection from the substrate, the other from the epitaxial layer. Figure 1 is the simulation of the rocking curves of $In_{0.52}Ga_{0.48}As/InP$ single heterostruc-

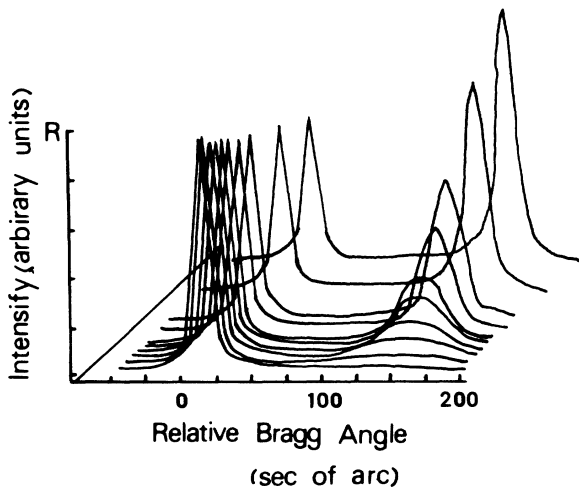


FIG. 1. Theoretical rocking curves of the uniformly single layers with different thickness. Cu $K\alpha_1$ radiation and 004 reflection are assumed.

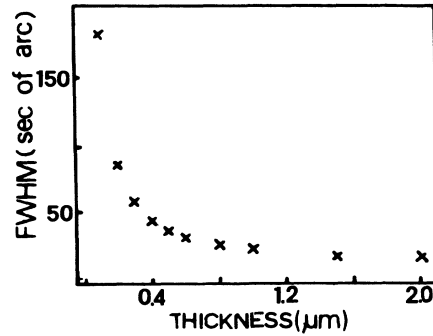


FIG. 2. FWHM of uniformly single layers vs thickness of layers.

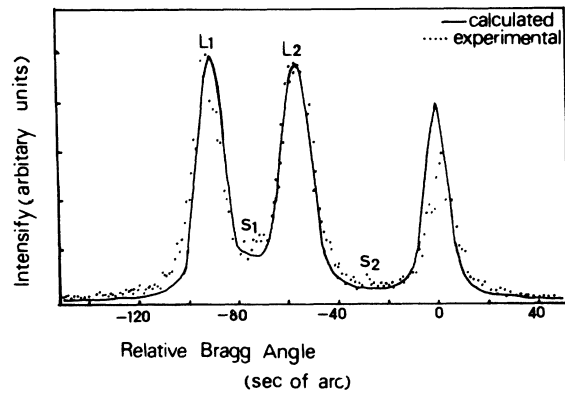


FIG. 3. Rocking curves of an $Al_{0.15}Ga_{0.85}As(2.5 \mu m)/GaAs$ waveguide structure and their simulation; Cu $K\alpha_1$ 004 reflection.

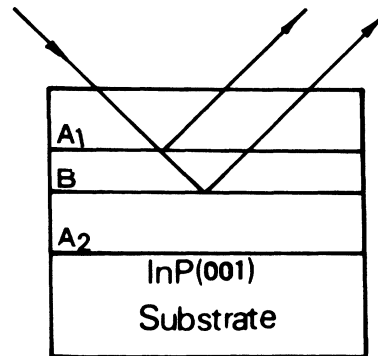


FIG. 4. Graph of a laser double heterostructure, $In_xGa_{1-x}As/InP$.

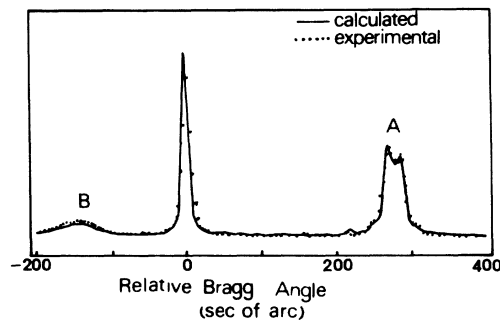


FIG. 5. Rocking curves and their simulations of an $In_xGa_{1-x}As/InP A_1BA_2$ specimen on position 4; Cu $K\alpha_1$ 004 reflection.

TABLE I. Growth and optimum simulating parameters of a waveguide specimen.

	Growth		Simulation	
	Layer thickness (μm)	Compositions	Layer thickness (μm)	Compositions
First layer	2.5	0.25	2.5	0.26
Second layer	1.5	0.15	1.7	0.16

tures with thicknesses from 0.1 to 2 μm . The surface normal of the specimens is [001]. One can see from Fig. 1 that as the thickness of layers increases, the intensity of the epitaxial layer increases and that of the substrate decreases. Moreover, the former even exceeds the latter when the thickness of the layer is more than 1 μm . This reflects the fact that x-ray energy in crystal is conserved in x-ray dynamical theory. On the contrary in x-ray kinematical theory the diffracting intensities are independent of the thickness of specimens. Figure 2 shows the variation of the full width at half maximum (FWHM) of the reflecting peaks of epitaxial layers with the thickness of layers. It is obvious that the ω (FWHM) versus t (thickness) curve is hyperbolalike and has the following relationship:

$$\omega = cscht. \quad (5)$$

For the epitaxial layers with superior quality Eq. (5) can be employed to measure the thickness of the layers.

B. Structures of waveguide

Epitaxial structures for waveguide devices often consist of two or more epilayers. The rocking curve and the simulation of an $\text{Al}_x\text{Ga}_{1-x}\text{As}/\text{GaAs}$ waveguide structure are shown in Fig. 3. Table I shows the growth parameters, comparing with those of the simulated ones. From Table I one can see that the nominal growth parameters are different from the experimental values. The theoretical parameters chosen to match the experimental values are the true parameters.

C. Laser structures

Laser structures often consist of two layers of the same composition A_1 above and A_2 below the active layer of a different composition B . Because of the existence of the

active layer B the reflecting waves from A_1 and A_2 result in a phase shift and interfere with each other. For this reason the peak related to A_1 and A_2 will become asymmetric or even split into two peaks. Theoretical and experimental results show that the interference induced by the active layer is dependent upon the composition and the thickness of B . The fine structures of the A peak are very sensitive to the variation of the composition and thickness of B .^{13,14}

Figure 4 shows a laser double heterostructure ($\text{In}_x\text{Ga}_{1-x}\text{As}/\text{InP}$). The growth parameters of A_1 , B and A_2 are shown in Table II. In order to study the homogeneities along the surface of the specimen, four different positions on the surface, denoted by 1, 2, 3, and 4, respectively, were examined. Figure 5 shows the experimental rocking curve and its simulation on position 4. The simulating parameters are shown in Table II. It is clearly shown from Fig. 5 that the simulated curve is in good agreement with the experimental one. Both curves exhibit similar substructure and asymmetric splitting in A peaks. As the A peaks include the interference induced by B layers, the studies of the fine structures of A peaks will give useful information about the B layer. One can think that the variation of the rocking curves is mainly restricted by the inhomogeneities of the compositions. Figure 6 shows the distribution of the composition and mismatch at four positions on the surface of the specimen. The position of the peak of B is sensitive to the composition variation of layer by 50 ppm, and the compositional change of 10 ppm will lead to the modification of the A peak to be observed, it is concluded that simulating the fine structures of the A peak is a unique method to determine the compositional homogeneities of the layer B .

D. Superlattices

The peaks of the rocking curves of the superlattices which are complicated are not simply related to the

TABLE II. Growth and optimum simulating parameters of a laser structure at position 4 of the specimen.

Layer (from substrate)	Growth			Simulation		
	Thickness (μm)	Composition	Mismatch (ppm)	Thickness (μm)	Composition	Mismatch (ppm)
$A_1 \text{In}_x\text{Ga}_{1-x}\text{As}$	1	0.5160	-1100	0.78	0.5160	-1100
$B \text{In}_x\text{Ga}_{1-x}\text{As}$	0.25	0.5404	600	0.24	0.5403	591
$A_2 \text{In}_x\text{Ga}_{1-x}\text{As}$	0.25	0.5160	-1100	0.213	0.5160	-1100

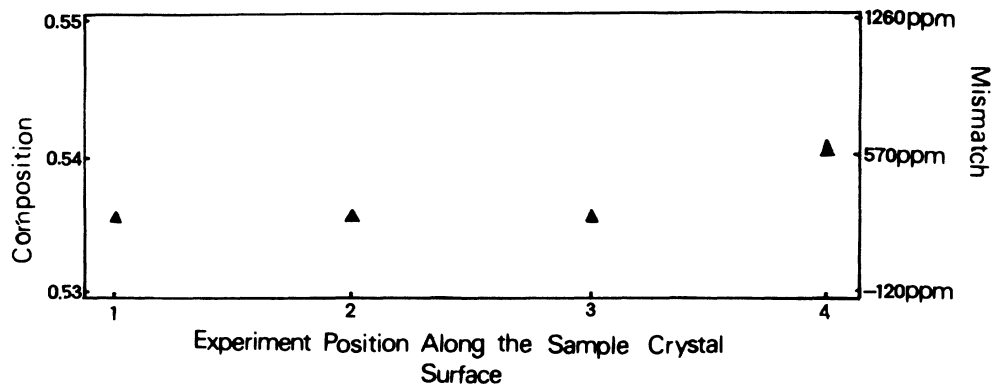


FIG. 6. Distribution of the composition and mismatch along the surface of the $\text{In}_x\text{Ga}_{1-x}\text{As}/\text{InP } A_1B A_2$ specimen.

mismatch of the lattice constants. To explain the rocking curves, theoretical simulations are therefore needed.

Figure 7 shows the experimental and theoretical rocking curves of 004 diffraction of $\text{In}_{0.15}\text{Ga}_{0.85}\text{As}(70 \text{ \AA})/\text{GaAs}(100 \text{ \AA})$ superlattices with 15 periods. A symmetrical reflection geometry of 422 was used for the first crystal to obtain a σ polarization beam. In the $\text{In}_x\text{Ga}_{1-x}\text{As}/\text{GaAs}$ system because of the large mismatch the growing interface will be no longer coherent when x exceeds a critical value $x_c=0.11$.¹⁵ Therefore for $\text{In}_{0.15}\text{Ga}_{0.85}\text{As}/\text{GaAs}$ the interface will be relaxed partly. Let γ be the percentage of relaxation, then the coherent growth region is $1-\gamma$, the lattice constant can be calculated approximately by

$$d'_1 = \gamma a_0 + (1-\gamma)d_{\perp},$$

where a_0 is the lattice constant of material, and d_{\perp} is the perpendicular constant deduced from tetragonal distortion. When $\gamma=50\%$, the theoretical and experimental curves are in good agreement for Fig. 7. Table III shows the growth and optimum simulating parameters. For the $\text{In}_x\text{Ga}_{1-x}\text{As}/\text{GaAs}$, because of the large lattice mismatch, the growth interfaces are often not coherent even if the mismatch layers are very thin, which is less than 100 \AA in the present case, and the growth parameters are not easily controlled. Therefore the optimum simulating parameters represent the actual structure of specimens.

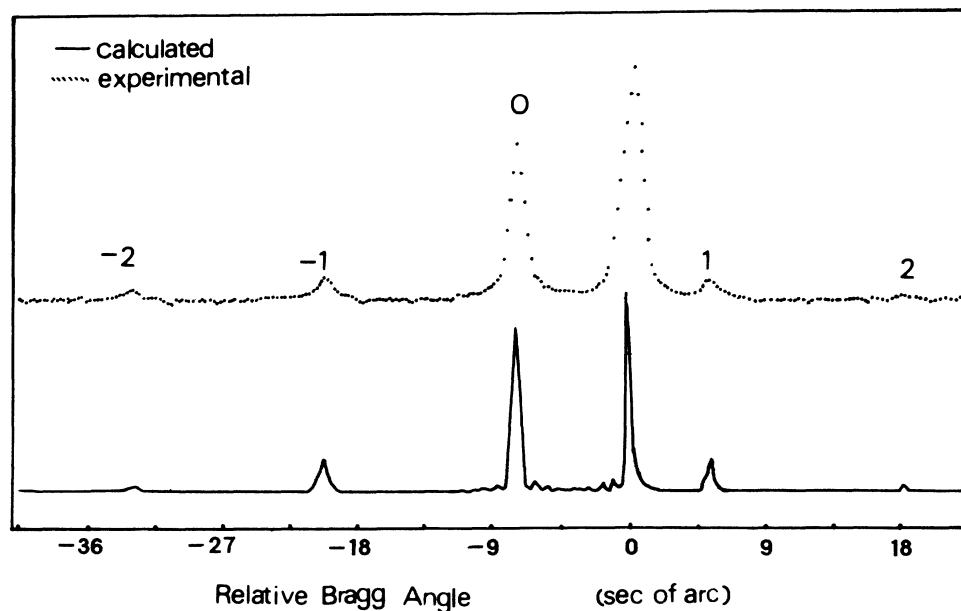


FIG. 7. Experimental rocking curves and their simulations of a superlattice of $\text{In}_{0.15}\text{Ga}_{0.85}\text{As}/\text{GaAs}$. $\text{Cu } K\alpha_1$ and 004 reflection are used. The first crystal is (211) single crystal of silicon and 422 reflection is accepted.

TABLE III. Growth and optimum simulating parameters of an $\text{In}_x\text{Ga}_{1-x}\text{As}(t_1)/\text{GaAs}(t_2)$ superlattice (15 periods).

	Growth	Simulation
x	0.15	0.12
t_1	70 Å	68 Å
t_2	100 Å	85 Å

IV. CONCLUSIONS

As described above, several device structures have been examined based upon our theoretical results. The theoretical results agree well with the experimental ones.

It is confirmed that Eq. (2) is applicable to arbitrary epitaxial structures. From the computer simulation of the x-ray double crystal diffraction rocking curves of epitaxial materials, a lot of useful information and the accurate structural parameters about epilayers are obtained which are significant for improving the quality and selecting the optimum growth conditions of device structures of III-V compound semiconducting materials.

ACKNOWLEDGMENT

The authors would like to thank Prof. Zhou Jun-ming for providing the specimens. The project is supported by the National Natural Science Foundation of China.

- ¹P. V. Petrashen, *Fiz. Tverd. Tela (Leningrad)* **16**, 2168 (1974) [*Sov. Phys.—Solid State* **16**, 1417 (1975)].
²P. V. Petrashen, *Fiz. Tverd. Tela (Leningrad)* **17**, 2814 (1975) [*Sov. Phys.—Solid State* **17**, 1882 (1976)].
³A. F. Afanasev *et al.*, *Phys. Status Solidi A* **42**, 415 (1975).
⁴R. N. Kyutt, P. V. Petrashen, and L. M. Sorokin, *Phys. Status Solidi A* **60**, 381 (1980).
⁵L. Tapfer and K. Ploog, *Phys. Rev. B* **33**, 5565 (1986).
⁶D. Taupin and J. Burgeat, *Acta Crystallogr., Sect. A* **24**, 99 (1968).
⁷A. Fukahara and Y. Takano, *Acta Crystallogr., Sect. A* **33**, 137 (1977).
⁸B. C. Larson and J. F. Barhorst *J. Appl. Phys.* **51**, 3181 (1980).

- ⁹M. A. G. Halliwell, M. H. Lyons, and M. J. Hill, *J. Cryst. Growth* **68**, 523 (1984).
¹⁰M. J. Hill, B. K. Tanner, M. A. G. Halliwell, and M. H. Lyons, *J. Appl. Cryst.* **18**, 446 (1985).
¹¹W. J. Bartels, J. Hornstra, and D. J. W. Lobeek, *Acta Crystallogr., Sect. A* **42**, 539 (1986).
¹²D. Taupin, *Bull. Soc. Fr. Minéral Cristallogr.* **87**, 469 (1969).
¹³X. Chu and B. K. Tanner, *Appl. Phys. Lett.* **49**, 1773 (1986).
¹⁴Cui Shu-fan and Mai Zhen-hong, *J. Appl. Cryst.* (to be published).
¹⁵Li Cheng-ji, Wang Yu-tian, and Ren Qing-yu, The 5th National Symposium on Surface and Interface Physics, Lanzhou, China, 1988 (unpublished).